A Simple and Cost-effective Method to Increase the Capacity of Carbon Nanotube sheet cathodes for Lithium-air Batteries

Keita Ushijima[1], Shinichiroh Iwamura[2], Shin R. Mukai[2]*

[1] Graduate School of Chemical Science and Engineering, Hokkaido University, N13W8, Kita-ku, Sapporo 060-6828, Japan.

[2] Faculty of Engineering, Hokkaido University, N13W8, Kita-ku, Sapporo 060-6828, Japan.

KEYWORDS

Carbon nanotube, Carbon nanofiber, Lithium-air battery, Oxygen permeability, Cathode

ABSTRACT

Thin sheets for the cathode of lithium-air batteries were prepared from a mixture of long carbon nanotubes and a fibrous carbon with a larger diameter. These sheets were found to have sufficient strength and high inner permeability. The discharge capacity of the sheets tended to increase with the decrease in their gas permeation resistance. The sheet with an optimized structure showed a high capacity, 17.7 mAh cm^{-2} at 0.1 mA cm^{-2}, and a moderate rate performance, 9.3 mAh cm^{-2} at 0.5 mA cm^{-2}. Analysis of the sheets after discharging revealed that improving the permeability of the sheets through the introduction of large pores by fibrous carbon addition leads to a significant improvement in cathode performance.

1. Introduction

Recently, energy storage devices are widely used in various applications, from smartphones, robots, drones to electric vehicles (EVs). The spread of EVs is expected to be the key to tackle environmental issues, therefore the EV market is rapidly growing. Presently, energy storage devices used for EVs are mainly lithium-ion batteries. As their energy density is only about 100-150 Wh kg^{-1} [1], the cruising distance of EVs is limited to half that of gasoline or hybrid vehicles. As methods to improve the energy density of lithium-ion batteries is limited [2], the development of further powerful energy storage devices is required to increase the cruising distance of EVs. Lithium-air batteries (LABs) are expected to become the key battery system of the next-generation due to their high theoretical energy density of around 11140 Wh kg^{-1}, which is about 10 times larger than that of lithium-ion batteries [3-4].

LABs generate energy through the following reactions:

$$(\text{cathode})\ 2Li^+ + O_2 + 2e^- \leftrightarrows Li_2O_2$$

$$(\text{anode})\ Li \leftrightarrows Li^+ + e^-$$

During discharging, oxygen supplied to the cathode from the atmosphere reacts with lithium-ions provided from the anode, and Li_2O_2 is deposited in the cathode. During subsequent charging, Li_2O_2 is decomposed to lithium-ions and oxygen which is the opposite of the discharge reaction. The cathode in this system needs to have a high surface area, permeability, and electrical conductivity to respectively provide a sufficient surface area for Li_2O_2 deposition, enable smooth oxygen transfer, and enable smooth electron transfer. To increase discharge capacity, it is also important to increase the void volume in the cathode. As the discharge reaction will terminate when deposits block the diffusion paths within the cathode, it is also important to maintain paths to the voids until they are completely filled with Li_2O_2.

Porous carbons with a high surface area such as graphene [2, 5-7], carbon blacks [8-10], carbon gels [11-12], and carbon nanotubes (CNTs) [13-16] are typically used as the cathode material. However, as it is difficult to construct a three-dimensional conducting network only from them, they are usually combined with current collectors such as carbon papers or metal meshes. Although such current collectors occupy a large ratio of the weight and volume of the cathode, they can hardly contribute to charge/discharge reactions due to their insufficient surface area. Therefore, if the usage of such current collectors can be avoided, the energy density of LABs can be significantly increased.

It has been reported that sheets that can be easily prepared through simple vacuum filtration of a suspension containing CNTs [17-19] can be used as a LAB cathode without an additional current

collector. Such sheets only have a moderate surface area, but as voids corresponding to meso- or macro-pores are naturally formed within them, a large discharge capacity can be achieved when they are used as the cathode, since the capacity is largely affected by the volume of meso-macro pores rather than surface area [11, 20-22]. However, commercially available CNTs are still too expensive for industrial applications. Carbon nanofibers (CNFs) are relatively inexpensive but their aspect ratio (= length/ diameter) is generally too small for them to be formed into sheets without the aid of a binder. On the other hand, CNFs with a high aspect ratio, which can be efficiently produced through the liquid pulse injection (LPI) technique [23], can be easily formed into sheets.

The LPI technique can also be used to synthesize CNTs with a high aspect ratio. It has been reported that the discharge capacity of LPI-CNT sheets is twice larger than that of a cathode composed of a carbon paper and carbon black [19]. Nevertheless, the volume of deposited Li_2O_2 corresponding to the reported capacity is only about 30% of the total void volume existing in the LPI-CNT electrode. As discharge terminates when the diffusion paths of oxygen within the electrode are blocked with deposits, improving the oxygen permeability of the electrodes by introducing macro-pores is thought to be effective to increase discharge capacity. It has been reported that the introduction of macro-pores by using poly(methyl methacrylate) particles with a diameter of 6-27 μm and polystyrene particles with a diameter of 50 or 385 nm as the template increased discharge capacity to approximately 1.8 times that of the same material without macropore introduction [24-25]. However, the preparation of such electrodes requires an additional process step to remove the templates. Moreover, it is difficult to maintain the strength of such electrodes, and the introduction of large macropores tends to reduce the energy density of the cathode, as they are not effective to store Li_2O_2. Therefore, the development of a simple and

inexpensive technique to improve the permeability of the electrodes is required to obtain high capacity cathodes. The permeability of CNF sheets can be improved by increasing the diameter of the CNFs used to prepare it. However, it becomes difficult to obtain sheets from CNFs when their diameter is increased, as the increase in diameter is usually accompanied by a decrease in aspect ratio. Indeed there is a unique CNF production method, electrospinning, which allows the production of CNFs with a high aspect ratio. However, it is difficult to obtain CNFs with a diameter small enough to provide the minimum surface area required for it to be used as a LAB cathode material [26]. In this study, attempts were made to obtain sheets from fibrous carbons with a moderate strength and surface area, and also through which oxygen can easily diffuse. Our strategy was to combine CNTs with an aspect ratio high enough to enable easy sheet fabrication, with a fibrous carbon with a larger diameter to introduce large voids to improve the oxygen permeability of the resulting sheet. Using the obtained sheets the relationship between cathode performance and the properties of the sheets was investigated.

2. Experimental

2.1 LPI-CNT/CNF production

CNTs with an average diameter of 3 nm (CNT3) and CNFs with an average diameter of 80 nm (CNF80) were produced through the LPI technique according to a previous report [23]. Figure 1 shows a schematic illustration of the experimental apparatus used for the LPI technique. The length and inner diameter of the ceramic reactor were 1200 mm and 85 mm, respectively. The initial source for CNT3 production was a mixture of benzene, ferrocene, thiophene, and methanol (all reagents were purchased from FUJIFILM Wako Pure Chemical Co.) with a weight ratio of

14:1.5:0.3:84.2, respectively. The reactor was heated to 1200°C using an electric furnace under a H_2 flow of 17.6 cm min^{-1}. The initial source was injected from the top of the reactor as liquid pulses of 100 µL $pulse^{-1}$ for 120 times at intervals of 30 s. Then, the produced CNT3 was collected from the bottom of the reactor after the reactor was cooled down to room temperature.

For the production of CNF80, the initial source was changed to a mixture of benzene, ferrocene, and thiophene with a weight ratio of 94:5:1, respectively. The flow rate of H_2, total pulse number, and injection interval were also changed to 7.2 cm min^{-1}, 30 times, and 60 s, respectively.

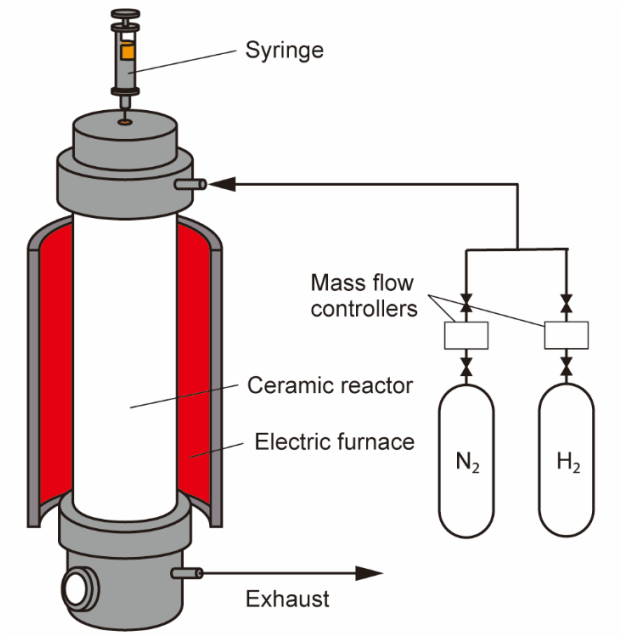

Figure 1 Schematic illustration of the apparatus for LPI-CNT/CNF production.

2.2 Sheet fabrication

CNT sheets, prepared only from CNT3 (CNT3(100)) was fabricated according to a previous report [19]. Ten mg of CNT3 was stirred in 20 mL of ethylene glycol (FUJIFILM Wako Pure Chemical Co.) for 2 hours. This suspension was vacuum-filtered using a hydrophobic poly(tetrafluoroethylene) membrane (H010A025A, pore size: 0.1 μm, effective diameter: 16 mm, Advantec), and the sample was washed with 20 mL of ethanol. The sheet sample was dried at room temperature yielding CNT3(100).

CNF12 with an average diameter of 12 nm, CNF30 with an average diameter of 30 nm and CF10,000 (CF = carbon fiber) with an average diameter of 10 μm were purchased from Sigma-Aldrich Japan, Tokyo Chemical Industry and Mitsubishi Chemical Co., respectively. CNT3 and a fibrous carbon with a larger diameter (CNF12, CNF30, CNF80 or CF10,000) were stirred in 20 mL of ethylene glycol at a fixed mixing ratio (total amount: 10 mg). The sheets were fabricated from the suspension through the same process used for CNT3(100) fabrication. The resulting sheets were represented using the mixing ratio, for example CNT3(20)-CNF80(80) indicates that the sheet was prepared from 20wt% of CNT3 and 80wt% of CNF80.

2.3 Characterization

The fibrous carbons used in this work and cross-sections of the sheets obtained from them were observed by a field-emission scanning electron microscope (SEM, JSM-6500F; JEOL) and a transmission electron microscope (TEM, JEM-2010; JEOL). Elemental mappings of the electrodes were conducted using an energy dispersive X-ray spectrometer equipped with a SEM (SEM-EDX, FSM-6510LA; JEOL). Stress-strain diagrams were obtained by applying stress using an universal testing apparatus (AG-100kNXplus; Shimazu) to specimens (3 cm x 1 cm) cut out from the sheets.

To measure the electric conductivity of the sheets, ribbon-shaped samples with a width of about 1 cm were cut out from the sheets. A conductive Ag paste (Dotite D-500; Fujikura Kasei) was applied to both ends of the sample, and the ends were connected to a potentiostat (HA-151; Hokuto Denko). Various voltages were applied to the sample, and the resulting current values were recorded to obtain I-V diagrams. The electrical conductivity was calculated from the slope of the I-V diagram. Nitrogen adsorption experiments of the fibrous carbons were conducted at -196°C using a gas adsorption apparatus (BELSORP mini; Microtrac BEL) to obtain adsorption isotherms. The BET surface area of the samples was calculated from the isotherms. Gas permeation resistance of the sheets was measured using a hand-made apparatus (an illustration of the apparatus is shown in the Supporting Information section). N_2 gas was passed through the specimen sheets to obtain flow rate vs. pressure drop diagrams. Gas permeation resistance (R_{gp} [Pa cm^2/(cm^3 h^{-1} cm)]) was calculated from the slope of the diagrams using the following equation:

$$R_{\mathrm{gp}} = \frac{\Delta P \times A}{L \times d}$$

Where ΔP [Pa] is the pressure drop, A [cm^2] is the cross-section area, L [cm^3 h^{-1}] is the volumetric flow rate, and d [cm] is the sheet thickness.

2.4 Evaluation of LAB cathode performance

2032-type coin cells having small holes on the cathode cap to allow oxygen supply were assembled in an Ar-filled glove box using the synthesized sheets, lithium foil, and a glass microfiber filter (GF/A; Whatman) as the cathode, anode, and separator, respectively. CF_3SO_3Li in tetraglyme ether (1:4, molar ratio) was used as the electrolyte, and 100 μL of it was applied on

the separator during assembling,. The coin cells were set in a gas-tight box equipped with tubes. Through the tubes, oxygen was supplied into the box at a flow rate of 10 mL min^{-1}. The coin cells were galvanostatically discharged to 2.0 V and charged to 4.4 V at a current density of 0.1, 0.3 or 0.5 mA cm^{-2}. For comparison, typical electrodes (CP+KB), which were prepared from a carbon paper (CP, TGP-H-060; Toray) and Ketjen black (KB), were also measured. A paste obtained by mixing KB, polyvinylidene difluoride (PVDF) and N-Methyl-2-pyrrolidone (NMP) was applied to CP. The weight ratio between KB and PVDF was 19:1. After drying at 115°C under vacuum, circles with a diameter of 16 mm were punched out from the synthesized sheet to obtain CP+KB electrodes.

3. Results and discussion

3.1 Sheet Fabrication

Although it has been reported that CNFs with a low aspect ratio cannot be formed into a sheet [19], in this study, most mixtures of CNT3 and fibrous carbons could be formed into sheets which could be easily handled, even though the aspect ratios of the added fibrous carbons were fairly low. It was found that as CNT3 enables easy entanglement of the fibers due to its high aspect ratio, only 20wt% of it was required to form a stable sheet in most combinations. Only CNT3(20)-CNF12(80) had some apparent defects, probably due to the significantly low aspect ratio of CNF12. Figure 2 shows SEM and TEM images of CNT3 and CNF80, and cross-sectional SEM images of the electrodes prepared from mixtures of them. The cross-sectional SEM images and inset photographs of CNT3-CNF80 samples (Figure 2 c-e) show that CNTs and CNFs with different diameters were successfully formed into sheets. In addition, the existence of domains mostly formed by CNF80

can be confirmed in the resulting sheets. Such domains are expected to increase the permeability of the sheets.

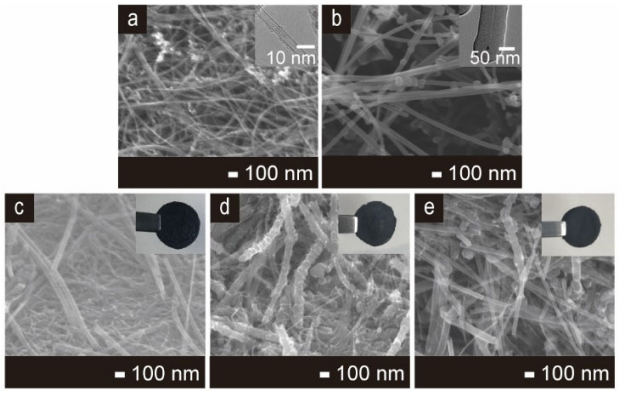

Figure 2 SEM images of CNT3 and CNF80 and sheets prepared by mixing them at different ratios. (a: CNT3, b: CNF80, c: CNT3(80)-CNF80(20), d: CNT3(50)-CNF80(50), e: CNT3(20)-CNF80(80), insets: TEM images(a,b) and photographs(c-e))

Physical properties, including the results of tensile strength tests and electric conductivity tests, of CP and sheets prepared by mixing CNT3 with CNF80 are summarized in Table 1. When the mixing ratio of CNF80 was increased, the sheet thickness tended to increase and the porosity consequently increased. CP has an elasticity of 534 MPa which value is significantly higher than those of the CNT3(100) and the sheets prepared by mixing CNT3 with CNF80 (maximum 29.1 MPa). This result indicates that CP had a rigid and inflexible structure, whereas the sheets prepared from CNT3 and CNF80 were quite flexible. This is because CNT3-CNF80 sheets were formed through the entanglement of thin fibers, and CP was formed from thick and stiff CFs using binders.

Moreover, the elasticity of the sheets decreased by increasing the mixing ratio of CNF80. The breaking stress of CNT3(100) (2.99 MPa) was equivalent to that of CP (2.75 MPa). While the breaking stress tended to decrease with the increase in the mixing ratio of CNF80, it can be regarded that such decreases will scarcely affect their handling ability. Strain energy decreased as the mixing ratio of CNF80 was increased. The lowest strain energy value of CNT3-CNF80 sheets (0.36 mJ) was higher than that of CP (0.12 mJ), indicating that CNT3-CNF80 sheets can bear tougher handling than CP. These results suggest that CNT3-CNF80 sheets have sufficient mechanical properties for electrode applications.

The electrical conductivity of CNT3-CNF80 sheets was mostly equivalent to or higher than that of CP (191 S cm^{-1}). CNT3(20)-CNF80(80) showed the lowest electrical conductivity of 29.8 S cm^{-1}, a value of which can still be regarded as sufficient for LAB cathodes. The purpose of mixing a fibrous carbons with a larger diameter is to improve the oxygen permeability of the cathode. To evaluate gas permeability, the permeation resistance the sheets cause when nitrogen was passed through them was measured. Figure 3 shows the gas permeation resistance of the electrodes. It can be noticed that as expected, the resistance decreases with the increase in the mixing ratio of the thicker fibrous carbon. These results suggest that the pores in the sheet were enlarged by aggregation of the thicker fibrous carbon. Considering that the porosity also increases with the increase in the mixing ratio, it is expected that oxygen can smoothly diffuse into sheets prepared at a high mixing ratio of the thick fibrous carbon when they are used as the cathode of LABs.

Table 1 Physical properties of the electrodes.

	Thickness [μm]	Porosity [%][a]	Elasticity [MPa]	Breaking stress [MPa]	Strain energy [mJ]	Electric conductivity [S cm^{-1}]
CP	190	78	534	2.75	0.12	191
CNT3(100)	210	86	26.6	2.99	1.66	298
CNT3(80)-CNF80(20)	210	87	29.1	3.93	2.72	254
CNT3(50)-CNF80(50)	250	89	14.9	0.951	0.57	243
CNT3(20)-CNF80(80)	290	91	5.97	0.463	0.36	29.8

a Calculated by the equation $\varepsilon = 100\text{-}\frac{4m}{\pi\rho_c d^2 L}\times 100$ (ε : porosity, m : weight of the sheet (10 mg), ρ_c : true density of carbon (2.0 g cm^{-3}), d : diameter of the sheet (16 mm), L : thickness of the sheet)

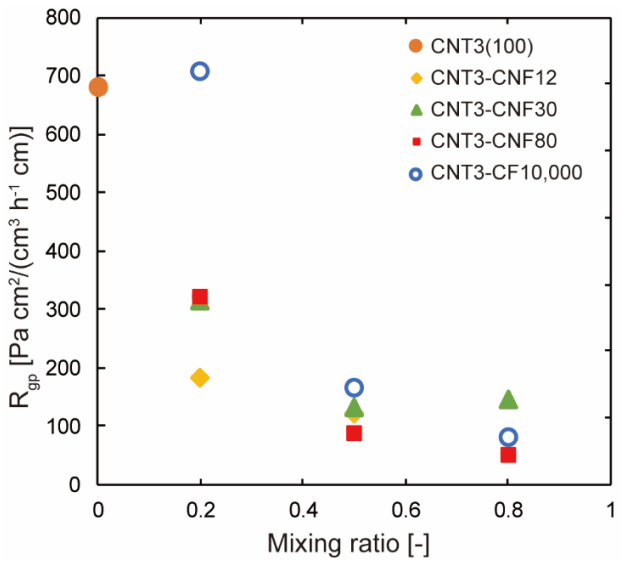

Figure 3 The relationship between the mixing ratio of a CNF/CF and the gas permeation resistance of sheets (R_{gp}) prepared by mixing it with CNT3.

3.2 Li_2O_2 storage property

The results of sheet property analysis described above revealed the potential of the sheets to be used as the cathode of LABs. Figure 4 shows the discharge curves of the sheets prepared by mixing CNT3 with CNF80. Each discharge curve showed a plateau between 2.5 and 2.7 V corresponding to the reaction of the deposition of Li_2O_2 [3]. The discharge capacity of the sheets tended to increase with the increase in the mixing ratio of CNF80. This is because the large voids formed by the addition of CNF80 improved the oxygen permeability of the cathode, and this led to the homogeneous deposition of Li_2O_2, or in other words efficient utilization of the space for Li_2O_2 storage. Even though these sheets can be prepared through a simple process, a high discharge capacity of 17.7 mAh cm^{-2} or 3540 mAh g^{-1} can be achieved, values of which are comparable to those of high-performance cathodes such as graphene electrodes[2], which generally can be obtained only through low productive processes. It should also be noted that the gravimetric discharge capacity is reported as the value per weight of the whole cathode, so it is much higher than that of typical cathodes made using powdery materials, such as Ketjen black[19], if the capacities are calculated based on the weight including the current collector. Only CNT3(80)-CNF80(20) showed a lower discharge capacity than CNT3(100). It is assumed that the pore enlargement effect of CNF80 was not sufficient in this sheet, as the amount of it was limited.

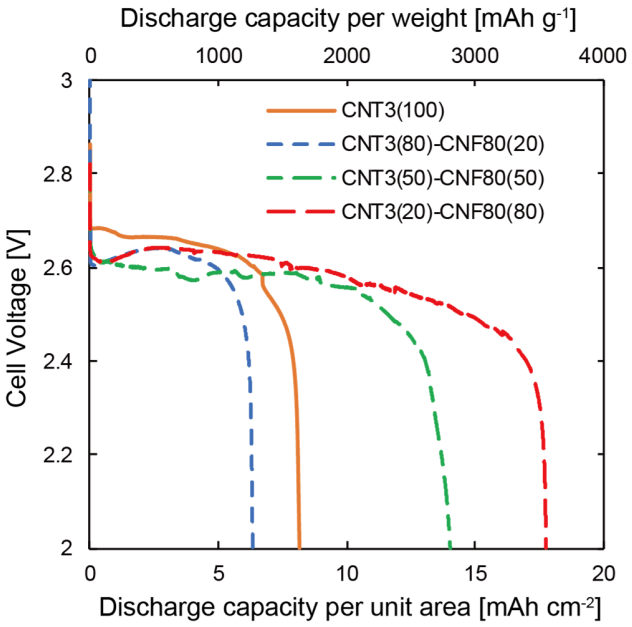

Figure 4 Discharge curves of CNT3(100) and sheets prepared from mixtures of CNT3 and CNF80. (Current density: 0.1 mA cm^{-2})

Figure 5 shows the discharge capacity of electrodes prepared by mixing CNT3 with CNFs/CFs with different diameters. The discharge capacity of electrodes prepared by mixing CNT3 with CNF12, CNF30, and CNF80 tended to increase gradually, as the mixing ratio of the thicker fiber was increased. Similarly, the discharge capacity of electrodes prepared by mixing CNT3 with CF10,000 increased with the increase in the mixing ratio of CF10,000 up to a ratio of about 50%, but it started to decrease when the mixing ratio was further increased. It is assumed that the surface area of CNT3(20)-CF10,000(80) was too low for efficient Li_2O_2 deposition. The surface areas of CNT3(50)-CF10,000(50) and CNT3(20)-CF10,000(80) estimated from the surface areas and mixing ratios of CNT3 and CF10,000 were 106 m^2g^{-1} and 71 m^2g^{-1}, respectively. Indeed, it has been reported that the surface area of the cathode is not a significantly important factor in LABs

[27], but the discharge capacity of cathodes with very low surface areas, such as CP, is extremely low. Moreover, it has also been reported that there is a limit in the discharge capacity of CNFs prepared via electrospinning owing to their low surface area [26]. Considering the surface area of CNT3(20)-CNF80(80) and CNT3(50)-CNF10,000(50) and their discharge capacities, it is assumed that the minimum surface area required for the cathode to show a sufficient discharge capacity is around 100 m^2g^{-1}. This indicates that fibrous carbons which are significantly less expensive than CNTs, such as CFs, can also be used to obtain a LAB cathode with a fairly high capacity, as long as their mixing ratio is properly adjusted. Therefore, it was shown that partial substitution of CNTs with less expensive fibrous carbons not only leads to capacity enhancement, but also to a significant reduction in the production cost of the cathode for LABs.

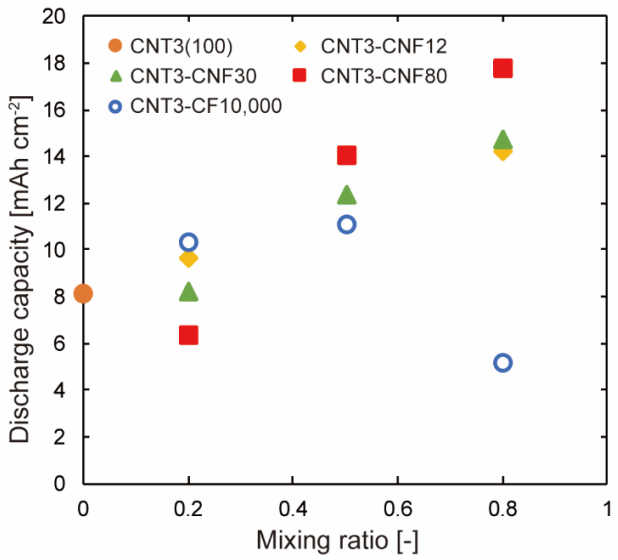

Figure 5 The relationship between the mixing ratio of a CNF/CF and the discharge capacity of electrodes prepared by mixing it with CNT3. (Current density: 0.1 mA cm^{-2})

3.3 Influence of permeability on discharge capacity

The above results indicate that partial substitution of CNTs in the sheets with a thicker fibrous carbon improved the oxygen permeability of the sheets, resulting in an increase in discharge capacity. The relationship between discharge capacity and gas permeability of the sheets was investigated. Figure 6 shows the relationship between discharge capacity and gas permeation resistance of the sheets with a sufficient specific surface area. The figure indicates that the discharge capacity increases with the decrease in gas permeation resistance. In particular, the discharge capacity of CNT3(20)-CNF80(80) was about twice that of CNT3(100). Interestingly, the discharge capacities of sheets with a similar gas permeation resistance were almost the same in spite of the type of fibrous carbon mixed with CNT3.

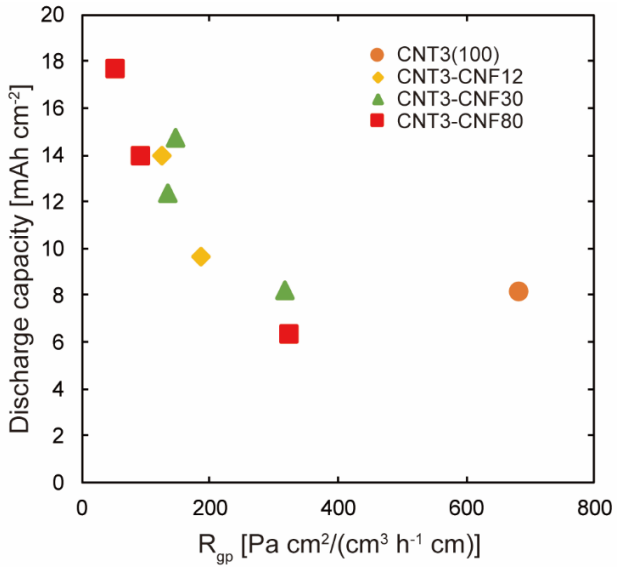

Figure 6 The relationship between gas permeation resistance and discharge capacity of the sheets prepared by mixing CNT and CNF. (Current density: 0.1 mA cm^{-2})

To investigate how the oxygen permeability affects the manner of Li_2O_2 deposition in the cathode, SEM-EDX analysis of the cross-section of cathode sheets after discharging was conducted. Prior to analysis, the sheets were sufficiently washed with tetraglyme ether and dried to remove the electrolyte. Figure 7 shows the results of cross-sectional oxygen mapping of CNT3(100) and CNT3(20)-CNF80(20) discharged to different depths. As the oxygen in the deposited Li_2O_2 is detected in this analysis, the figures show how Li_2O_2 is distributed within the sheets (see the Supporting Information section). In all the images shown in Figure 7, the top of the images corresponds to the oxygen inlet side and the bottom to the lithium metal anode (separator) side. Figure 7a,b shows that Li_2O_2 was homogeneously distributed in CNT3(100) at least until the cell was discharged to a depth of 7 mAh cm^{-2}, but when the cell was further discharged down to 2.0 V, selective deposition of Li_2O_2 at the oxygen inlet side could be confirmed. These results suggest that oxygen and lithium ions could smoothly diffuse within the sheet at least up to a discharge depth of about 7 mAh cm^{-2}, but after that, the deposited Li_2O_2 gradually starts to disturb diffusion, resulting in the selective deposition of Li_2O_2 where oxygen can easily gain access, the region close to the oxygen inlet side. Discharging will terminate when oxygen can no longer diffuse into the cathode. This mechanism agrees with previous reports [28-29]. In contrast, Li_2O_2 could be homogeneously deposited throughout CNT3(20)-CNF80(80) even when discharged down to 2.0 V, as shown in Figure 7c-e. These results suggest that the homogeneously deposited Li_2O_2 hardly hampered the diffusion of oxygen and lithium ions until the final stage of discharging, so a discharge capacity much higher than that of CNT3(100) could be achieved. From the above results, it can be concluded that the improvement of the oxygen permeability of the cathode by the introduction of large voids, leads to the promotion of homogeneous deposition of Li_2O_2, resulting

in an increase in discharge capacity. In CNT-based sheets, this can be easily achieved by simply mixing a fibrous carbon with a larger diameter.

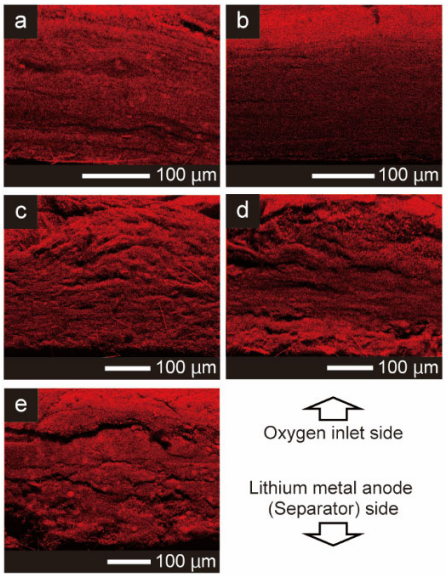

Figure 7 Cross-sectional oxygen mapping images of (a,b) CNT3(100) and (c-e) CNT3(20)-CNF80(80) after discharging to depths of (a,c) 7 mAh cm^{-2}, (d) 14 mAh cm^{-2} and (b,e) down to 2.0 V. (Current density: 0.1 mA cm^{-2})

*The top of the images corresponds to the oxygen inlet side and the bottom to the lithium metal anode (separator) side.

3.4 Rate performance

The results described above indicate that the electrical conductivity and gas permeability of the sheets prepared by mixing CNT3 with CNF80 differ according to the ratio between the two carbons.

Since these properties significantly affect rate performance, the rate performance of the sheets was evaluated. Figure 8 shows the discharge capacities of CNT3(100), CNT3(20)-CNF80(80), and CP+KB measured at different current densities. The discharge capacity of CP+KB, which is generally used as a standard cathode for LABs, measured at a low current density was significantly lower than sheets prepared from CNT3, or CNT3 and CNF80, and the capacity did not largely decrease when the current density was increased. This is because this electrode has significantly large voids which are provided by the CP. Such voids are effective to maintain oxygen permeability, but cannot contribute to efficient Li_2O_2 storage, as they are too large. In contrast, CNT3(100) and CNT3(20)-CNF80(80) showed high discharge capacities at a low current density, but the capacities largely decreased with the increase in current density due to clogging of oxygen inlets by Li_2O_2 deposition. CNT3(20)-CNF80(80) maintained half of its discharge capacity measured at 0.1 mA cm^{-2} even when the current density was increased to 0.5 mA cm^{-2}, indicating that the large voids introduced by CNF80 enabled smooth diffusion of oxygen during discharging even at fairly high current densities. The current density at which the discharge capacity of CNT3(20)-CNF80(80) starts to decrease was lower than that of CNT3(100), suggesting that the amount of Li_2O_2 deposition causing serious clogging was different and depends on sheet structure. In a previous report, a graphene cathode showed a discharge capacity of 41.1 mAh cm^{-2} at 0.1 mA cm^{-2} [2]. A CNT cathode showed a discharge capacity of 5.74 mAh cm^{-2} at 0.5 mA cm^{-2} [15]. Considering such reports, CNT3(20)-CNF80(80) can be regarded as a LAB cathode which can show high discharge capacities at high current densities. In addition to its cathode performance, the sheets can be expected to be used as a practical cathode for LABs as they can be easily produced at a low production cost.

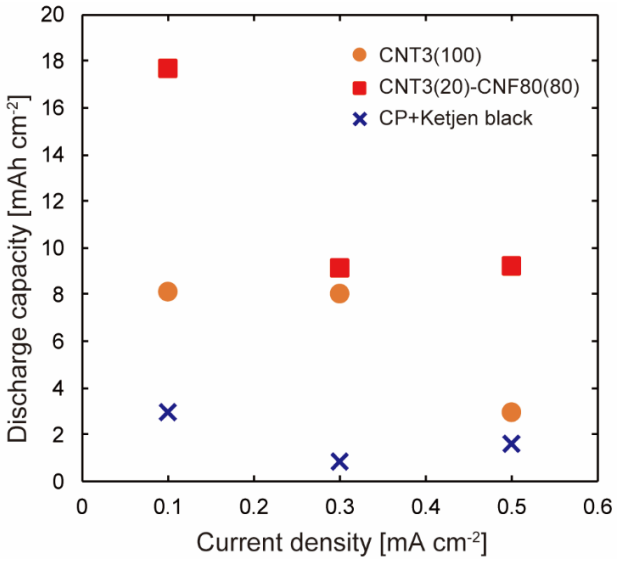

Figure 8 Rate performance of CNT3(100), CNT3(20)-CNF80(80), and CP+KB.

4. Conclusion

Sheet electrodes can be easily prepared from CNTs with a high aspect ratio but the structure of such sheets can be hardly tuned. Therefore, a simple and cost-effective method was developed to improve the gas permeation resistance of the sheets. In this method, CNTs were simply mixed with a thicker fibrous carbon, namely CNFs, which cannot be individually formed into sheets due to its low aspect ratio. Through this process, stable sheets can be obtained even when the weight ratio of the mixed CNFs is about 80%. Characterization of these sheets indicated that they possess strengths and conductivities comparable to commercially-available CP and sheets prepared only from CNTs with a high aspect ratio. Furthermore, the gas permeation resistance of the sheets was found to decrease with the increase in the mixing ratio of CNFs. By decreasing the gas permeation resistance of the sheets, their discharge capacities can be increased up to approximately twice their original value. The sheets also showed high capacities at high current densities. Such high

capacities and rate performances are thought to be obtained through the improvement of the oxygen permeability of the sheets. In addition to the high performance of the sheets, the production process of them is simple, and the total cost of the fibrous carbons used to obtain them is much cheaper than the case in which sheets are synthesized only from CNTs. Thus, the sheets can be expected to be used as a practical cathode in LABs because of not only their performance as a LAB cathode, but also as their productivity is high and production cost is low. Furthermore, considering their high strength, conductivity, surface area and gas permeability, it is expected that the sheets can be applied not only to LABs but also to various devices such as fuel cells, and redox flow batteries.

ASSOCIATED CONTENT

Supporting Information.

The Supporting Information is available free of charge.

Illustration of the apparatus to measure the gas permeation resistance; Evaluation of O-containing material in the discharged cathode (PDF)

AUTHOR INFORMATION

Corresponding Author

*E-mail: iwamura@eng.hokudai.ac.jp

ORCID

Shinichiroh Iwamura: 0000-0001-8827-8880

Shin R. Mukai: 0000-0003-2194-4513

Author Contributions

The manuscript was written through contributions of all authors. All authors have given approval to the final version of the manuscript.

Funding Sources

JST ALCA-SPRING Grant Number JPMJAL1301.

ACKNOWLEDGMENT

This study was partly supported by JST ALCA-SPRING Grant Number JPMJAL1301, Japan. A part of this study was conducted at Laboratory of XPS analysis, Joint-use facilities, Hokkaido University.

ABBREVIATIONS

EV, electric vehicle; LAB, lithium-air battery; CNT, carbon nanotube; LPI, liquid pulse injection; CF, carbon fiber; SEM, field-emission scanning electron microscope; TEM, transmission electron microscope; R_{gp}, gas permeation resistance; CP, carbon paper; KB, ketjen bleck; PVDF, polyvinylidene difluoride; NMP, N-methyl-2-pyrrolidone.

REFERENCES

(1) Mahlia, T. M. I.; Saktisandan, T. J.; Jannifar, A.; Hasan, M. H.; Matseelar, H. S. C. A review of available methods and development on energy storage; technology update. *Renew. Sust. Energ. Rev.* **2014,** *33*, 532-545, DOI: 10.1016/j.rser.2014.01.068.

(2) Lin, Y.; Moitoso, B.; Martinez-Martinez, C.; Walsh, E. D.; Lacey, S. D.; Kim, J. W.; Dai, L. M.; Hu, L. B.; Connell, J. W. Ultrahigh-Capacity Lithium-Oxygen Batteries Enabled by Dry-Pressed Holey Graphene Air Cathodes. *Nano Lett.* **2017,** *17* (5), 3252-3260, DOI: 10.1021/acs.nanolett.7b00872.

(3) Abraham, K. M.; Jiang, Z. A polymer electrolyte-based rechargeable lithium/oxygen battery. *J. Electrochem. Soc.* **1996,** *143* (1), 1-5, DOI: 10.1149/1.1836378.

(4) Xiao, J.; Mei, D. H.; Li, X. L.; Xu, W.; Wang, D. Y.; Graff, G. L.; Bennett, W. D.; Nie, Z. M.; Saraf, L. V.; Aksay, I. A.; Liu, J.; Zhang, J. G. Hierarchically Porous Graphene as a Lithium-Air Battery Electrode. *Nano Lett.* **2011,** *11* (11), 5071-5078, DOI: 10.1021/nl203332e.

(5) Li, Y. L.; Wang, J. J.; Li, X. F.; Geng, D. S.; Li, R. Y.; Sun, X. L. Superior energy capacity of graphene nanosheets for a nonaqueous lithium-oxygen battery. *Chem. Commun.* **2011,** *47* (33), 9438-9440, DOI: 10.1039/c1cc13464g.

(6) Yoo, E.; Zhou, H. S. Li-Air Rechargeable Battery Based on Metal-free Graphene Nanosheet Catalysts. *Acs Nano* **2011,** *5* (4), 3020-3026, DOI: 10.1021/nn200084u.

(7) Xin, X.; Ito, K.; Kubo, Y. Graphene/activated carbon composite material for oxygen electrodes in lithium-oxygen rechargeable batteries. *Carbon* **2016,** *99*, 167-173, DOI: 10.1016/j.carbon.2015.12.015.

(8) Beattie, S. D.; Manolescu, D. M.; Blair, S. L. High-Capacity Lithium-Air Cathodes. *J. Electrochem. Soc.* **2009,** *156* (1), A44-A47, DOI: 10.1149/1.3005989.

(9) Kubo, Y.; Ito, K. Multicell Stack of Nonaqueous Lithium-Air Batteries. *ECS Trans.* **2014,** *62*, 129-135, DOI: 10.1149/06201.0129ecst.

(10) Xu, W.; Viswanathan, V. V.; Wang, D.; Towne, S. A.; Xiao, J.; Nie, Z.; Hu, D.; Zhang, J.-G. Investigation on the charging process of Li2O2-based air electrodes in Li-O-2 batteries with organic carbonate electrolytes. *J. Power Sources* **2011,** *196* (8), 3894-3899, DOI: 10.1016/j.jpowsour.2010.12.065.

(11) Sakai, K.; Iwamura, S.; Mukai, S. R. Influence of the Porous Structure of the Cathode on the Discharge Capacity of Lithium-Air Batteries. *J. Electrochem. Soc.* **2017,** *164* (13), A3075-A3080, DOI: 10.1149/2.0791713jes.

(12) Mirzaeian, M.; Hall, P. J. Preparation of controlled porosity carbon aerogels for energy storage in rechargeable lithium oxygen batteries. *Electrochim. Acta* **2009,** *54* (28), 7444-7451, DOI: 10.1016/j.electacta.2009.07.079.

(13) Li, J.; Wang, N.; Zhao, Y.; Ding, Y.; Guan, L. MnO2 nanoflakes coated on multi-walled carbon nanotubes for rechargeable lithium-air batteries. *Electrochem. Commun.* **2011,** *13* (7), 698-700, DOI: 10.1016/j.elecom.2011.04.013.

(14) Li, Y.; Wang, J.; Li, X.; Liu, J.; Geng, D.; Yang, J.; Li, R.; Sun, X. Nitrogen-doped carbon nanotubes as cathode for lithium-air batteries. *Electrochem. Commun.* **2011,** *13* (7), 668-672, DOI: 10.1016/j.elecom.2011.04.004.

(15) Tan, P.; Shyy, W.; Wei, Z. H.; An, L.; Zhao, T. S. A carbon powder-nanotube composite cathode for non-aqueous lithium-air batteries. *Electrochim. Acta* **2014,** *147*, 1-8, DOI: 10.1016/j.electacta.2014.09.074.

(16) Zhang, T.; Zhou, H. From Li-O-2 to Li-Air Batteries: Carbon Nanotubes/Ionic Liquid Gels with a Tricontinuous Passage of Electrons, Ions, and Oxygen. *Angew. Chem. Int. Ed.* **2012,** *51* (44), 11062-11067, DOI: 10.1002/anie.201204983.

(17) Nomura, A.; Ito, K.; Kubo, Y. CNT Sheet Air Electrode for the Development of Ultra-High Cell Capacity in Lithium-Air Batteries. *Sci. Rep.* **2017,** *7*, DOI: 10.1038/srep45596.

(18) Chen, Y.; Li, F.; Tang, D.-M.; Jian, Z.; Liu, C.; Golberg, D.; Yamada, A.; Zhou, H. Multi-walled carbon nanotube papers as binder-free cathodes for large capacity and reversible non-aqueous Li-O-2 batteries. *J. Mater. Chem. A* **2013,** *1* (42), 13076-13081, DOI: 10.1039/c3ta11792h.

(19) Sakai, K.; Iwamura, S.; Sumida, R.; Ogino, I.; Mukai, S. R. Carbon Paper with a High Surface Area Prepared from Carbon Nanofibers Obtained through the Liquid Pulse Injection Technique. *Acs Omega* **2018,** *3* (1), 691-697, DOI: 10.1021/acsomega.7b01822.

(20) Kuboki, T.; Okuyama, T.; Ohsaki, T.; Takami, N. Lithium-air batteries using hydrophobic room temperature ionic liquid electrolyte. *J. Power Sources* **2005,** *146* (1-2), 766-769, DOI: 10.1016/j.jpowsour.2005.03.082.

(21) Ma, S. B.; Lee, D. J.; Roev, V.; Im, D.; Doo, S.-G. Effect of porosity on electrochemical properties of carbon materials as cathode for lithium-oxygen battery. *J. Power Sources* **2013,** *244*, 494-498, DOI: 10.1016/j.jpowsour.2013.03.150.

(22) Ding, N.; Chien, S. W.; Hor, T. S. A.; Lum, R.; Zong, Y.; Liu, Z. Influence of carbon pore size on the discharge capacity of Li-O-2 batteries. *J. Mater. Chem. A* **2014,** *2* (31), 12433-12441, DOI: 10.1039/c4ta01745e.

(23) Mukai, S. R.; Rikima, Y.; Furukawa, R.; Ogino, I. Analysis of the Growth Behavior of Carbon Nanofibers Synthesized Using the Liquid Pulse Injection Technique. *Ind. Eng. Chem. Res.* **2013,** *52* (44), 15281-15286, DOI: 10.1021/ie400526f.

(24) Shen, C.; Liu, T.; Zhang, M.; Hendrickson, M. A.; Plichta, E. J.; Zheng, J. P. Macroporous Carbon Nanotube (CNT) Foams as Li-Air Battery Cathodes. *ECS Trans.* **2017,** *77* (11), 239-248, DOI: 10.1149/07711.0239ecst.

(25) Kim, H.; Lee, H.; Kim, M.; Bae, Y.; Baek, W.; Park, K.; Park, S.; Kim, T.; Kwon, H.; Choi, W.; Kang, K.; Kwon, S.; Im, D. Flexible free-standing air electrode with bimodal pore architecture for long-cycling Li-O-2 batteries. *Carbon* **2017,** *117*, 454-461, DOI: 10.1016/j.carbon.2017.03.015.

(26) Nie, H.; Xu, C.; Zhou, W.; Wu, B.; Li, X.; Liu, T.; Zhang, H. Free-Standing Thin Webs of Activated Carbon Nanofibers by Electrospinning for Rechargeable Li-O-2 Batteries. *ACS Appl. Mater. Interfaces* **2016,** *8* (3), 1937-1942, DOI: 10.1021/acsami.5b10088.

(27) Read, J.; Mutolo, K.; Ervin, M.; Behl, W.; Wolfenstine, J.; Driedger, A.; Foster, D. Oxygen transport properties of organic electrolytes and performance of lithium/oxygen battery. *J. Electrochem. Soc.* **2003,** *150* (10), A1351-A1356, DOI: 10.1149/1.1606454.

(28) Bardenhagen, I.; Yezerska, O.; Augustin, M.; Fenske, D.; Wittstock, A.; Baeumer, M. In situ investigation of pore clogging during discharge of a Li/O-2 battery by electrochemical impedance spectroscopy. *J. Power Sources* **2015,** *278*, 255-264, DOI: 10.1016/j.jpowsour.2014.12.076.

(29) Bardenhagen, I.; Fenske, M.; Fenske, D.; Wittstock, A.; Baeumer, M. Distribution of discharge products inside of the lithium/oxygen battery cathode. *J. Power Sources* **2015,** *299*, 162-169, DOI: 10.1016/j.jpowsour.2015.08.089.

For Table of Contents Only